

# MHD Analysis in Hydromagnetic Casting Process of Clad Steel Slabs

Eiichi Takeuchi<sup>1)</sup>, Hiroshi Harada<sup>1)</sup>,  
Masafumi Zeze<sup>2)</sup>, and Hiroyuki Tanaka<sup>3)</sup>

1) Process Technology Research Labs, Nippon Steel, Chiba, Japan  
2) Yawata R&D Labs, Nippon Steel, Kitakyushu, Japan  
3) Yawata Works, Nippon Steel, Kitakyushu, Japan

## ABSTRACT

A novel continuous casting process for clad steel slabs has been developed by suppressing the mixing of molten steels in the mold pool of continuous casting strand with a level DC magnetic field (LMF) installed in the mold.

In this process, two molten steels of different chemical composition are discharged by two nozzles into the upper and the lower pools respectively to solidify in the outer and the inner layers as a clad steel slabs. The mechanism of the separation into two layers has been elucidated by using a three dimensional MHD analysis. The numerical prediction employing Maxwell's equation, Ohm's law, and the turbulent flow model shows that the mixing of the different type of steels is suppressed by the electromagnetic dividing of the upper and the lower recirculating flows. The principle of the new process has been also verified by steel casting trials of the stainless-steel clad steel slabs with an 8-ton scale pilot continuous casting machine.

## NOMENCLATURE

$A_1$  = cross-sectional area of outer layer ( $m^2$ )  
 $A_2$  = cross-sectional area of inner layer ( $m^2$ )  
 $A_T$  = total cross-sectional area ( $m^2$ )  
 $B$  = magnetic flux density (T)  
 $C$  = chemical concentration (%)  
 $E$  = electric field intensity (V/m)  
 $f_e$  = Lorentz force ( $N/m^3$ )  
 $D$  = diffusivity ( $m^2/s$ )  
 $d$  = thickness of solidifying shell (thickness of

outer layer)(m)

$H$  = magnetic field (A/m)  
 $J$  = induced current ( $A/m^2$ )  
 $K$  = solidification coefficient ( $mm/min^{0.5}$ )  
 $L$  = upper/lower pool boundary position (m)  
 $q$  = volumetric flow rate of molten steel corresponding to the amount of solidifying shell ( $m^3/s$ )  
 $Q_1$  = pouring rate into upper pool (kg/min)  
 $Q_2$  = pouring rate into lower pool (kg/min)  
 $Q_T$  = total pouring rate (kg/min)  
 $S$  = normalized concentration (%)  
 $s$  = unit area required to calculate the amount of solidifying shell ( $m^2$ )  
 $T$  = slab thickness (m)  
 $t$  = time (s)  
 $U$  = molten steel velocity (m/s)  
 $V_c$  = casting speed (m/min)  
 $W$  = slab width (m)  
 $\mu$  = magnetic permeability (H/m)  
 $\nu$  = kinematic viscosity ( $m^2/s$ )  
 $\rho_1$  = density of outer layer molten steel ( $kg/m^3$ )  
 $\rho_2$  = density of inner layer molten steel ( $kg/m^3$ )  
 $\rho_e$  = effective density of solidifying steel ( $kg/m^3$ )

## 1. INTRODUCTION

In recent years, technologies applying electromagnetic forces to material manufacturing processes have been remarkably advanced (Moffatt and Proctor, 1984), (Garnier, 1994), (Takeuchi et al., 1994). Through the study of the effect of a DC magnetic field with a level magnetic flux density in the width direction of the

continuous casting mold (called a level magnetic field and abbreviated to LMF) on the flow of molten steel in the mold by using mercury experiments and by performing a magnetohydrodynamic (MHD) analysis, the present authors found that the LMF can suppress the mixing of chemical composition in the mold pool (Takeuchi et al., 1991), (Zeze et al., 1993).

This finding induced the concept of the novel continuous casting process for clad steel slabs in which dissimilar molten steels in the mold pool are separated by LMF to solidify as a clad steel slab. The present study has been conducted in order to verify the principles of the proposed casting process for clad steel slabs by a three dimensional MHD analysis followed by experimental castings.

## 2. PRINCIPLE OF PROCESS

The continuous casting process of clad steel slab with the LMF is schematically illustrated in Fig. 1 (Takeuchi et al., 1994), (Takeuchi, 1995). The LMF is imposed on the lower part of the mold. Two molten steels of different chemical compositions are simultaneously supplied through short and long submerged entry nozzles into the upper and lower pools in the mold, respectively. By imposing DC magnetic field, the resultant braking force (Lorentz force) is expected to act on the flows to

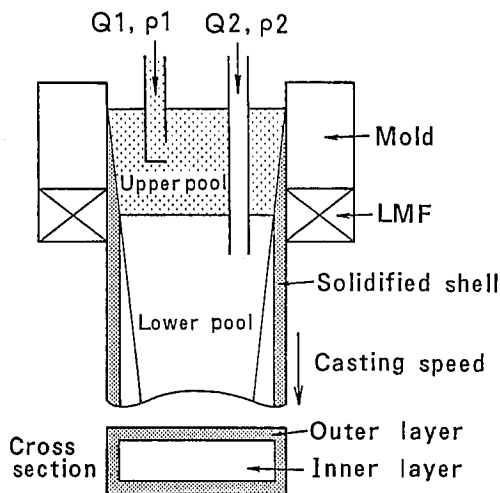


Fig. 1 Principle of continuous casting process for clad steel slabs with LMF.

prevent the mixing of the molten steels in the mold and magnetohydrodynamically divides the mold pool into upper and lower parts with the LMF as the boundary. Cooling through the water-cooled copper mold and water spray below the mold solidifies the molten steel in the upper pool between the meniscus and the LMF into the outer layer of the clad steel slab and the molten steel in the lower pool from the LMF down into the inner core of the clad steel slab.

The rates  $Q_1$  and  $Q_2$  at which the molten steels are poured into the upper and lower pools are the same as the rates at which the molten steels are consumed as the solidifying shell in the upper and lower pools, respectively. These rates are expressed by

$$Q_1 = \rho_1 A_1 V_C \quad (1)$$

$$Q_2 = \rho_2 A_2 V_C \quad (2)$$

where  $\rho_1$  and  $\rho_2$  are the densities of the solidifying steels in the upper and the lower pools, respectively;  $A_1$  and  $A_2$  are the cross-sectional areas of the outer and the inner layers, respectively; and  $V_C$  is the casting speed.

If  $T$ ,  $W$  and  $d$  are the mold thickness, mold width and outer layer thickness, respectively,

$$A_1 = WT - (W - 2d)(T - 2d) \quad (3)$$

$$A_2 = (W - 2d)(T - 2d) \quad (4)$$

Assuming that the growth of the solidifying shell in the mold follows the parabolic law, the outer layer thickness  $d$  is expressed by the following equation, using the distance  $L$  from the meniscus to the upper/lower pool boundary and the casting speed  $V_C$ :

$$d = Kt^n = K(L/V_C)^n \quad (5)$$

where  $t$  is time from the start of solidification;  $K$  is the solidification coefficient; and  $n$  is a time exponent that indicates the mold cooling characteristics.

The pouring rates into the upper and lower pools must be controlled to keep the upper/lower pool boundary level at the midheight of the LMF in terms of casting speed, mold size and mold cooling characteristics. The total pouring rate

$Q_T$  for both of the outer and inner layers must meet the following relationship:

$$\begin{aligned} Q_T &= Q_1 + Q_2 \\ &= \rho_e A_T V_c \\ &= \rho_e (WT) V_c \end{aligned} \quad (6)$$

where  $A_T$  is the total cross-sectional area of the slab; and  $\rho_e$  is the effective density of steel that allows for the bulging and shrinkage of the slab during casting.

### 3. MHD ANALYSIS

The mechanism of the suppression of mixing in the mold with the LMF in this process was analyzed by a three-dimensional MHD model. The MHD model is basically composed of governing equations for the magnetic field and flow field.

Assuming that the liquid metal is an incompressible fluid and is uniform and isotropic in electrical properties, the motion of the fluid is described by

$$\text{div } \mathbf{U} = 0 \quad \dots(7)$$

$$\frac{\partial \mathbf{U}}{\partial t} + (\mathbf{U} \cdot \text{grad}) \mathbf{U} = -\frac{1}{\rho} \text{grad } p + \nu \nabla^2 \mathbf{U} + \mathbf{g} + \frac{1}{\rho} \mathbf{f}_e \quad \dots(8)$$

The electromagnetic field is expressed by Maxwell's equations under magnetohydrodynamic approximations (Hughes and Young, 1966).

$$\text{Rot } \mathbf{E} = -\frac{\partial \mathbf{B}}{\partial t} = -\mu \frac{\partial \mathbf{H}}{\partial t} \quad \dots(9)$$

$$\text{rot } \mathbf{H} = \mathbf{J} \quad \dots(10)$$

$$\text{rot } \mathbf{B} = 0 \quad \dots(11)$$

Ohm's law in the molten metal moving at the velocity  $\mathbf{U}$  is given by

$$\mathbf{J} = \sigma (\mathbf{E} + \mathbf{U} \times \mathbf{B}) \quad \dots(12)$$

Since the fluid velocity is low in general, the magnetic Reynolds number of the system is smaller enough than unity. This means that the effect of fluid flow on the electromagnetic field is negligible. As the electric field  $\mathbf{E}$  is conservative, it can be represented by using the scalar potential  $\phi$  as follows:

$$\mathbf{E} = -\text{grad } \phi \quad \dots(13)$$

The equation of continuity of electric current is derived from Eq. (10):

$$\text{div } \mathbf{J} = 0 \quad \dots(14)$$

From Eqs. (12) to (14), the equations governing the electromagnetic field can be reduced into the following Poisson's equation:

$$\text{div grad } \phi = \text{div } \sigma (\mathbf{U} \times \mathbf{B}) \quad \dots(15)$$

The Lorenz force induced in the molten metal is given by

$$\mathbf{f}_e = \mathbf{J} \times \mathbf{B} = \sigma (-\text{grad } \phi + \mathbf{U} \times \mathbf{B}) \times \mathbf{B} \quad \dots(16)$$

Eqs. (7), (8), (15), and (16) were solved, subject to the initial and boundary conditions, using implicit finite difference method. The velocity fields were computed with the  $k-\epsilon$  model, in which the wall function and the free slip condition were employed at the solidification front and at the meniscus, respectively.

The mixing of solute element in the strand pool is simulated by the diffusion equation (17).

$$\frac{\partial C}{\partial t} + (\mathbf{U} \cdot \text{grad}) C = \text{div } D \text{ grad } C \quad \dots(17)$$

The nodal system for the computation is shown in Fig. 2.

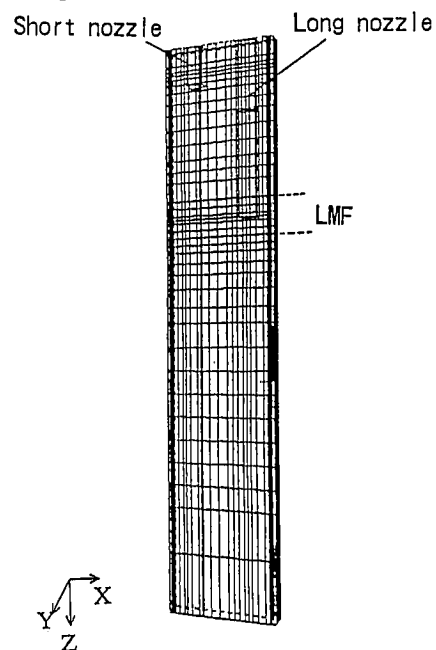


Fig. 2 Nodal system for numerical prediction

The solidifying shell was taken into account (Yoneyama et al., 1990) regarding the electric boundary condition.

For shell growth, the molten steel was absorbed from the nodal elements at the solidification front in the amount  $q_i$ , corresponding to the amount of solidification expressed by Eq. (18).

$$Q_i = \frac{d(t_{i+1}) - d(t_i)}{t_{i+1} - t_i} ds \quad \dots(18)$$

$$d(t_i) = 2.58 \times 10^{-3} t_i^{1/2} \quad \dots(19)$$

The following computational assumptions were made;

- i) The clad steel slab is continuously cast in the steady state.
- ii) The outer and inner layers have the same physical properties and temperature.
- iii) There is no slip on the solidifying shell surface and the nozzle surface.
- iv) The slab outside surface and the nozzle wall are electrically insulated.

Figure 3 shows the electric potential, induced electric current density and Lorentz force distributions in a clad steel slab continuously cast by applying an LMF. The electric current induced by the LMF and flow is greater on the inner layer nozzle side, and so is the resultant Lorentz force. It is understood that the suppression of mixing by the LMF is mainly due to the effect of the LMF in braking the

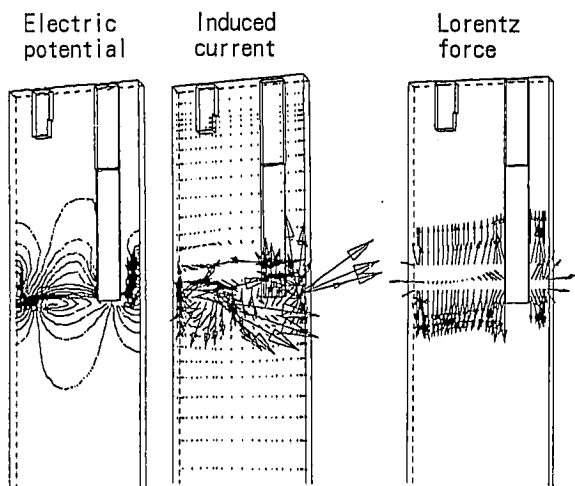


Fig. 3 Electric potential, induced electric current density and Lorentz force distributions as analyzed by MHD model.

discharging flow from the long nozzle in the lower pool.

The fluid flow and solute concentration distributions in the mold pool as calculated by the MHD model are shown in Fig. 4. When the LMF is not imposed, the molten steel flows generated by pouring into the upper pool and into the lower pool overlap in the mold pool and form a large circulating flow pattern, and the molten steels for outer and inner layers are mixed. When the LMF of 0.5 T is imposed, the above-mentioned circulating flow pattern is separated by the LMF, and circulating flow patterns are independently formed in each of the upper and lower pools. In the region where the LMF is applied, a stagnant area is formed, and the vertical flow of the molten steels in this region or

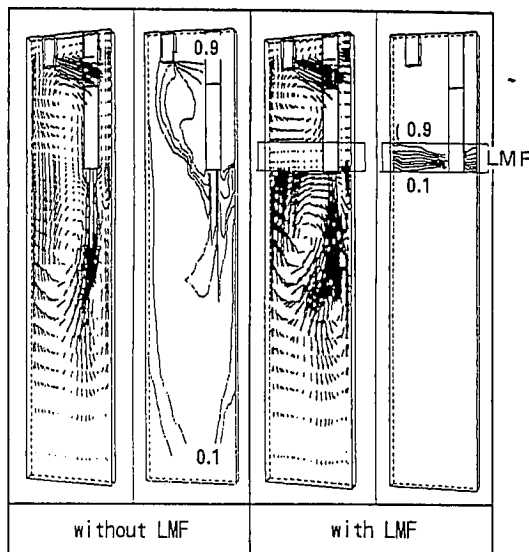


Fig. 4 Flow and solute concentration distribution as analyzed by MHD model.

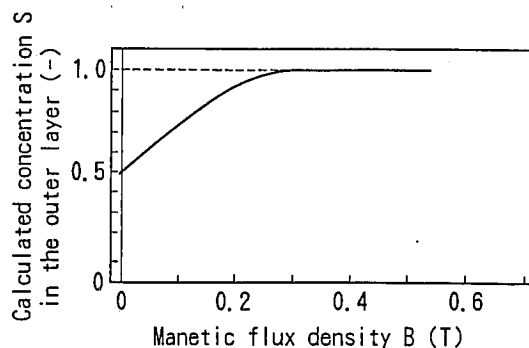


Fig. 5 Effect of magnetic flux density on the separation of solute element as calculated by MHD model.

mixing of the molten steels in the upper and lower pools is almost completely suppressed.

Figure 5 shows the effect of the LMF magnetic flux density on the separation of solute concentration in the mold pool as calculated by the MHD model. When the magnetic flux density is 0.3 T or more, the upper and lower pools are clearly divided, and the good separation of chemical component between the outer and inner layers is achieved.

## 4. EXPERIMENTAL CASTING

### 4.1 Experimental Apparatus and Procedure

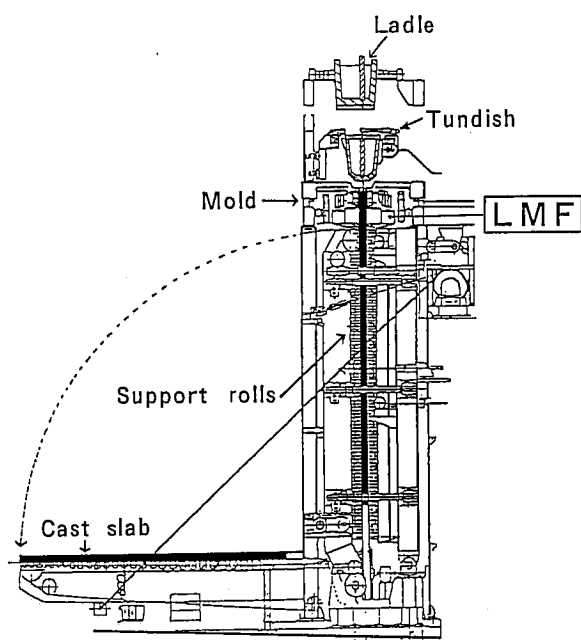


Fig. 6 Experimental slab caster.

Table 1 Experimental casting conditions.

Mold size	170 × 800 mm
Location of LMF core, L	470 ~ 710 mm from meniscus
Magnetic flux density, B	0 ~ 0.8 T
Casting speed, Vc	0.8 ~ 1.2 m/min
Casting length	8 m max.
Superheat in tundish	20 ~ 50 °C

Table 2 Chemical composition of stainless clad steel (mass%).

Layer	Grade	C	Si	Mn	P	S	Al	Cr	Ni	Ti
Outer	SUS304	0.015	0.45	0.85	0.015	0.005	0.01	10.5	18.5	---
Inner	Ti-SULC	0.003	0.02	0.20	0.010	0.005	0.04	---	---	0.02

The continuous caster used in the casting experiments is a vertical caster with a machine length of 8 m. It is schematically illustrated in Fig. 6 and its main specifications are given in Table 1.

Two tundishes are equipped with load cells capable of weighing the molten steel, so that the pouring rates of the molten steels into the inner and outer layers can be accurately measured and controlled.

A clad steel slab with outer and inner layers of stainless steel and low carbon steel, respectively, was continuously cast to verify the principle of the proposed process. The chemical composition of steels are listed in Table 2. The casting speed was 0.8 to 1.2 m/min., the magnetic flux density of the LMF was 0 to 0.8 T, and the upper/lower pool boundary position was located at 590mm from the meniscus.

### 4.2 Experimental Results

The cross-sectional macrostructures of stainless steel clad steel slabs are shown in Fig. 7. When a clad steel slab was cast without the LMF, the boundary between the outer and inner layers is not clearly distinguishable as shown in Fig. 7 (a). This means that the molten steels for the outer and inner layers were mixed in the mold. When a clad steel was cast with the LMF, the boundary between the outer and inner layers is clearly distinguishable in terms of solidification structure as shown in Fig. 7 (b), and the outer layer thickness is practically uniform. It is presumed

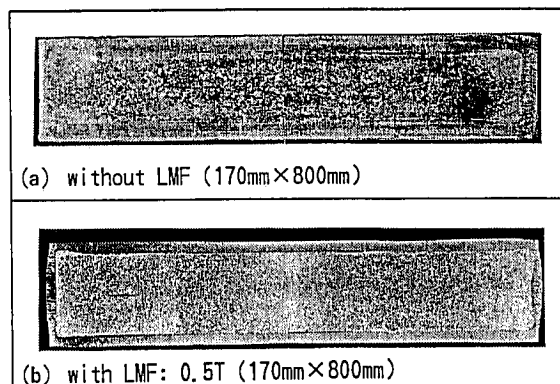


Fig. 7 Macrostructures of transverse sections of clad steel slabs cast without and with LMF.

that the boundary between the upper and lower pools was held almost horizontal.

The nickel concentrations in clad steel slabs in the thickness direction as measured by an X-ray microanalyzer are shown in Fig. 8. The nickel concentrations in the outer and inner layers of the clad steel slab cast with the LMF are approximately equal to those in the molten steels in the tundishes for the outer and inner layers, respectively. Good separation of chemical composition between the outer and inner layers is thus confirmed.

Figure 9 shows the effect of the LMF magnetic flux density on the separation of chemical component as investigated when clad steel slabs were continuously cast at the speed of

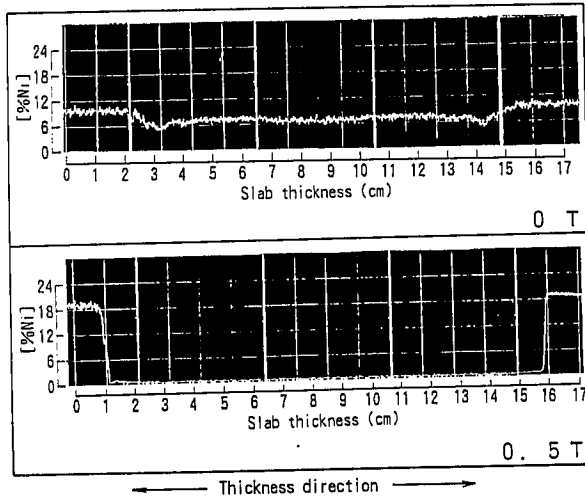


Fig. 8 Nickel concentrations in clad steel slabs in thickness direction as measured by X-ray microanalyzer.

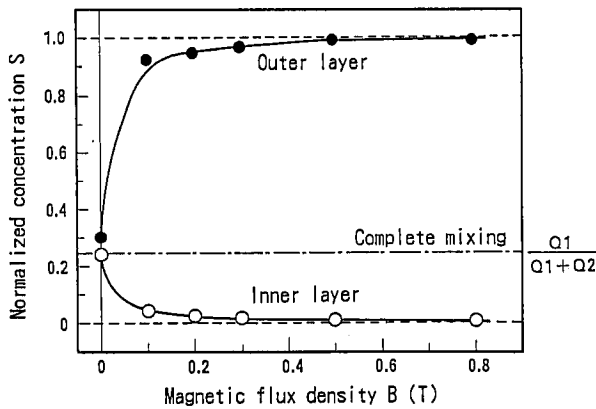


Fig. 9 Effect of magnetic flux density on separation of chemical composition. ( $V_c=1.0\text{m/min}$ ,  $L=590\text{mm}$ ,  $\Delta\rho=\rho_1-\rho_2=-0.22\text{g/cm}^3$ )

1.0 m/min with the boundary between the upper and lower pools held constant at the midheight of the LMF or at 590 mm from the meniscus. The separation of chemical component is evaluated by the normalized concentration  $S_x$  defined as follows:

$$S_x = \frac{C_x - C_2^0}{C_1^0 - C_2^0} \quad \dots(20)$$

where  $C_x^0$  is the solute concentration in the tundish;  $C_x$  is the solute concentration in the slab; and 1 and 2 denote the outer and inner layers of the slab, respectively. According to Eq. (20),  $S_1 = 1$  and  $S_2 = 0$  for complete separation of chemical composition, and  $S_1 = S_2 = Q_1/Q_t$  for complete mixing of chemical composition.

Since the solute concentrations in the outer and inner layers of the slab are almost constant in the thickness and circumferential directions as already described, the solute concentrations at 10 and 40 mm below the surface at the midwidth of the slab are used as representative solute concentrations of the outer and inner layers, respectively, to calculate the normalized concentrations  $S_x$ .

As shown in Fig. 9, increasing the magnetic flux density of the LMF increases the normalized concentration  $S_1$  in the outer layer, decreases the normalized concentration  $S_2$  in the inner layer, and improves the separation of chemical composition between the outer and inner layers. The corrosion resistant clad steel slabs with the normalized concentration  $S_1$  of 0.95 or more in the outer layer and the  $S_2$  of 0.05 or less in the inner layer can be produced when the magnetic flux density is 0.2 to 0.3 T or more. These results are in consistent with the numerical predictions.

## 5. CONCLUSIONS

In the process of hydromagnetic continuous casting of clad steel slabs, the two different compositions of liquid steel simultaneously discharged are divided into the upper and the lower pool by a level DC magnetic field, which solidify as the outer and the inner layer of clad

slabs, respectively. The hydromagnetic separation in the strand pool was numerically verified by a three dimensional MHD model prior to casting experiments. Calculated results showed that the DC magnetic field suppresses the mixing of solute element in the pool by braking the discharging flow from the submerged entry nozzles. The critical magnetic field density for the separation is about 0.3T.

The results of experimental casting of 18-8 stainless steel clad steel slabs are in good agreement with the numerical predictions ; (1) Clad steel slab has a uniform thickness of outer layer, which is well separated from the inner layer in terms of chemical composition, (2) The critical magnetic flux density of the LMF required to achieve the good separation of chemical composition between the outer and the inner layer is 0.2~0.3T.

#### REFERENCES

- Garnier, M., 1994, "Present and Future Prospect in Electromagnetic Processing of Materials", *Proc. International Symposium on Electromagnetic Processing of Materials*, Nagoya, Japan, pp.1-8.
- Hughes, W.F. and Young, F.J., 1966, *The Electromagnetohydrodynamics of Fluids*, John Wiley & Sons, pp.148.
- Moffatt, H.K. and Proctor, M.R.E., 1984, *Metallurgical Application of Magnetohydrodynamics*, The Metals Society, London.
- Takeuchi, E., Harada, H., Tanaka, H. and Kajioka, H., 1991, "Suppression of Mixing in the Pool of Continuous Casting Strand by DC Magnetic Field", *Magnetohydrodynamics in Process Metallurgy*, TMS., pp.261-266.
- Takeuchi, E., Tanaka, H. and Kajioka, H., 1994, "Hydromagnetic Separation of Metal Pool in the Continuous Casting Strand", *Proc. International Symposium on Electromagnetic Processing of Materials*, Nagoya, Japan, pp.364-371.
- Takeuchi, E., Toh, T., Harada, H., Zeze, M., Tanaka, H., Hojo, M., Ishii, T. and Shigematsu, K., 1994, Advances of Applied MHD Technology for Continuous Casting Process. *Nippon Steel Technical Report*, 61, pp.29-37.
- Takeuchi, E., 1995, Applying MHD Technology to the Continuous Casting of Steel Slab. *Journal of Metals*, pp.42-45.
- Yoneyama, Y., Takeuchi, E., Matsuzawa, K., Sawada, I., Hattori, Y. and Kishida, Y., 1990, Study on Electromagnetic Brake of Molten Steel Flow. *Nippon Steel Technical Report*, 45, pp.30-38.
- Zeze, M., Harada, H., Takeuchi, E. and Ishii, T., 1993, Application of a DC Magnetic Field for the Control of Flow in the Continuous Casting Strand. *Iron & Steelmaker*, 20, pp.53-57.

